OUKA
Osaka University Knowledge Archive

Title	Microstructure of Plasma-Sprayed Yttria-Stabilized Zirconia(Materials, Metallurgy & Weldability)
Author(s)	Iwamoto, Nobuya; Makino, Yukio; Endo, Shigeki
Citation	Transactions of JWRI. 1985, 14(1), p. 83-88
Version Type	VoR
URL	https://doi.org/10.18910/6232
rights	
Note	

Osaka University Knowledge Archive : OUKA

https://ir.library.osaka-u.ac.jp/

Osaka University

Microstructure of Plasma-Sprayed Yttria-Stabilized Zirconia

Nobuya IWAMOTO*, Yukio MAKINO** and Shigeki ENDO***

Abstract

Microstructures of plasma-sprayed YSZ before and after heat-treatment (1500°C, 1773 K) were investigated by XPS and SAM. Heterogeneity of yttrium was detected in the as-sprayed YSZ. Further, it is found that the heterogeneity disappears by the heat-treatment at 1500°C (1773 K). Binding energy of O_{1s} was strongly affected by the heterogeneity of yttrium and the splitting of O_{1s} peak was observed in yttrium-enriched region.

KEYWORDS: (Microstructure) (XPS) (SAM) (YSZ) (Plasma-Spraying)

1. Introduction

Various methods of surface treatment such as CVD and PVD have been performed for improving the properties of metals and alloys. Among these surface treatments, plasma spraying technique shows some advantages for versatile deposition of ceramics on metal substrates. Ceramic coating by plasma spraying have been widely used for the materials in ocean development and aircraft manufacturing and fairly successes have been obtained for improving the corrosion- and thermal-resistances of base materials [1–3]. Zirconia coating is one of the most available and promising ceramics, so that thermal characteristics of plasma sprayed zirconias on bond coat such as NiCrAlY have been investigated by many investigators [4–6]. Structure of various zirconias stabilized by some oxides have been elucidated by TEM and XRD methods, related to phase transition or order-disorder phenomenon. In this study, microstructure of plasma-sprayed yttria-stabilized zirconia on SUS 316 stainless steel investigated by XPS and AES methods.

2. Experimentals

Material used for plasma spraying was commercial YSZ (METCO 202) and SUS 316 stainless steel plates were used as substrate metal. One side of each steel plate was blasted just before plasma spraying. Plasma spraying equipment used was METCO 7M type and plasma spraying equipment was operated at 500 A and 65-70V using argon (0.04 m^3/min) and hydrogen (7.5 cm^3/min) gases as primary and secondary ones. Spraying distance was fixed as 6.4 cm. All other conditions were selected according to METCO technical bulletin.

XRD measurement was performed by following conditions;

Target: Cu K_α, Detector: S.C., Path: Air,
Voltage and current: 35 KV x 10 mA.

XPS spectra were measured using ESCA Lab-5 system (VG Scientific Co.) under a vacuum of 1×10^{-7}Pa or higher. Charging effect was corrected using electron neutralization so as to fit the peak position of C_{1s} of adsorbed carbon in every specimen to standard position of C_{1s} of hydrocarbon (284.6 eV). Spectra of C_{1s} were always measured before and after measuring the spectrum of a particular element. The conditions of electron neutralization were selected so that the peak position of C_{1s} spectrum is located at 284.6 eV within the accuracy of ±0.1 eV.

Scanning auger micrographs were taken using a spectrometer of PHI-545 type, operating at 3 KV and line scan speed of 1.5 sec under a vacuum of 1×10^{-7} Pa or higher.

3. Results

X-ray diffraction results of plasma sprayed zirconias and their powder before spraying are shown in Fig. 1. The

* Professor
** Instructor
*** Graduate Student, Metallurgical Engineering, Faculty of Engineering, Osaka University

Transactions of JWRI is published by Welding Research Institute of Osaka University, Ibaraki, Osaka 567, Japan

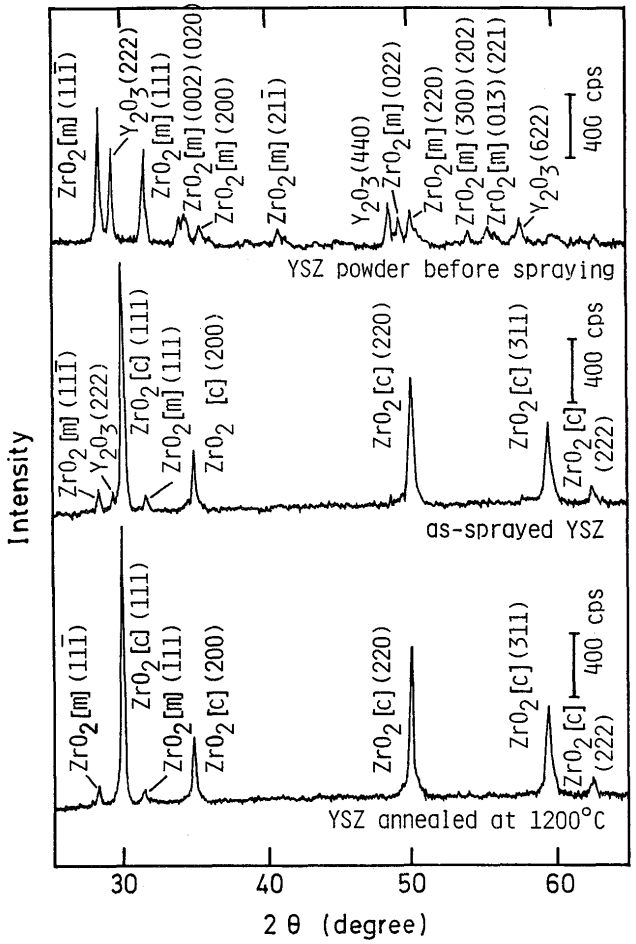

Fig. 1 X-ray diffraction patterns of YSZ powder, as-sprayed and annealed YSZs.

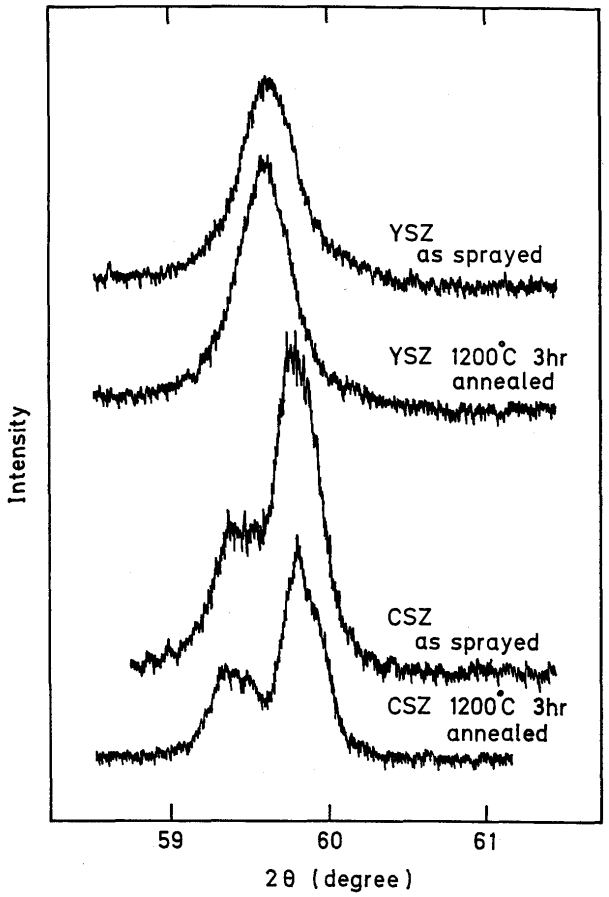

Fig. 2 X-ray diffraction peaks of (311) plane obtained from as-sprayed and annealed YSZ. (X-ray diffraction peaks of (311) plane obtained from as-sprayed and annealed CSZ are also illustrated.)

commercial YSZ is identified as a mixture of monoclinic zirconia and yttria before spraying whereas as-sprayed YSZ was identified as cubic zirconia containing small amount of monclinic zirconia and yttria. After heat-treatment at 1500°C (1773 K) for 3 hr (10.8 ks), the peak of yttria disappeared completely but the peaks due to monoclinic zirconia still remain. Enlarged profiles of (311) peaks obtained from cubic zirconias before and after heat-treatment at 1500°C (1773 K) are given in Fig. 2. The peak of (311) plane showed somewhat narrower width after heat-treatment. The profiles of (311) plane of plasma-sprayed CSZ were also illustrated in Fig. 2 in comparison with the result of plasma-sprayed YSZ.

Depth profiles of sprayed zirconias before and after heat-treatment are shown in Fig. 3. The ordinates in these profiles were taken by relative intensities $I(O_{1s})/I(Zr_{3p(1/2)})$[=R(O)] and $I(Y_{3d})/I(Zr_{3p(1/2)})$, respectively. Dumping in these depth profiles becomes small after heat-treatment. Dumping in the depth profiles before heat-treatment became small after heat-treatment except surface layer. Typical XPS spectra of O_{1s}, Zr_{4p} and Y_{3d} binding energies before and after heat-treatment at 1500°C (1773 K) are shown in Fig. 4. In fig. 4-(a), XPS spectra of three main elements at the positions having different R(O) value are shown in order of R(O) value. Further, splitting of O_{1s} peak was observed at the sputtering time of 12.3 ks (205 min). On the other hand, the splitting of O_{1s} peak was observed in the plasma-sprayed YSZ heat-treated at 1500°C (1773 K). Dependences of chemical shifts of O_{1s}, Y_{3d} and Zr_{4p} peak on R(O) value, are weak in the plasma-sprayed YSZ heat-treated at 1500°C (1773 K) compared with those in as-sprayed YSZ. Fig. 5 shows auger micrographs of main peaks observed at 110 eV, 153 eV and 177 eV. The peaks observed at 110 eV and 153 eV in the as-sprayed YSZ were identified as Y_{MNN} and Zr_{MNN} though these values are different from standard one. The peak observed at 177 eV remains unclear. In the plasma-sprayed YSZ heat-treated at 1500°C (1773 K), Zr_{MNN} peak was observed at 140 eV. As shown in fig. 5, distribution of zirconium was homogeneous in heat-treated YSZ compared with that in as-sprayed YSZ.

4. Discussions

It is shown from figs. 1 and 2 that mixture of monoclinic zirconia and yttria changes almost to cubic zirconia by plasma spraying process. Heat-treatment at 1200°C

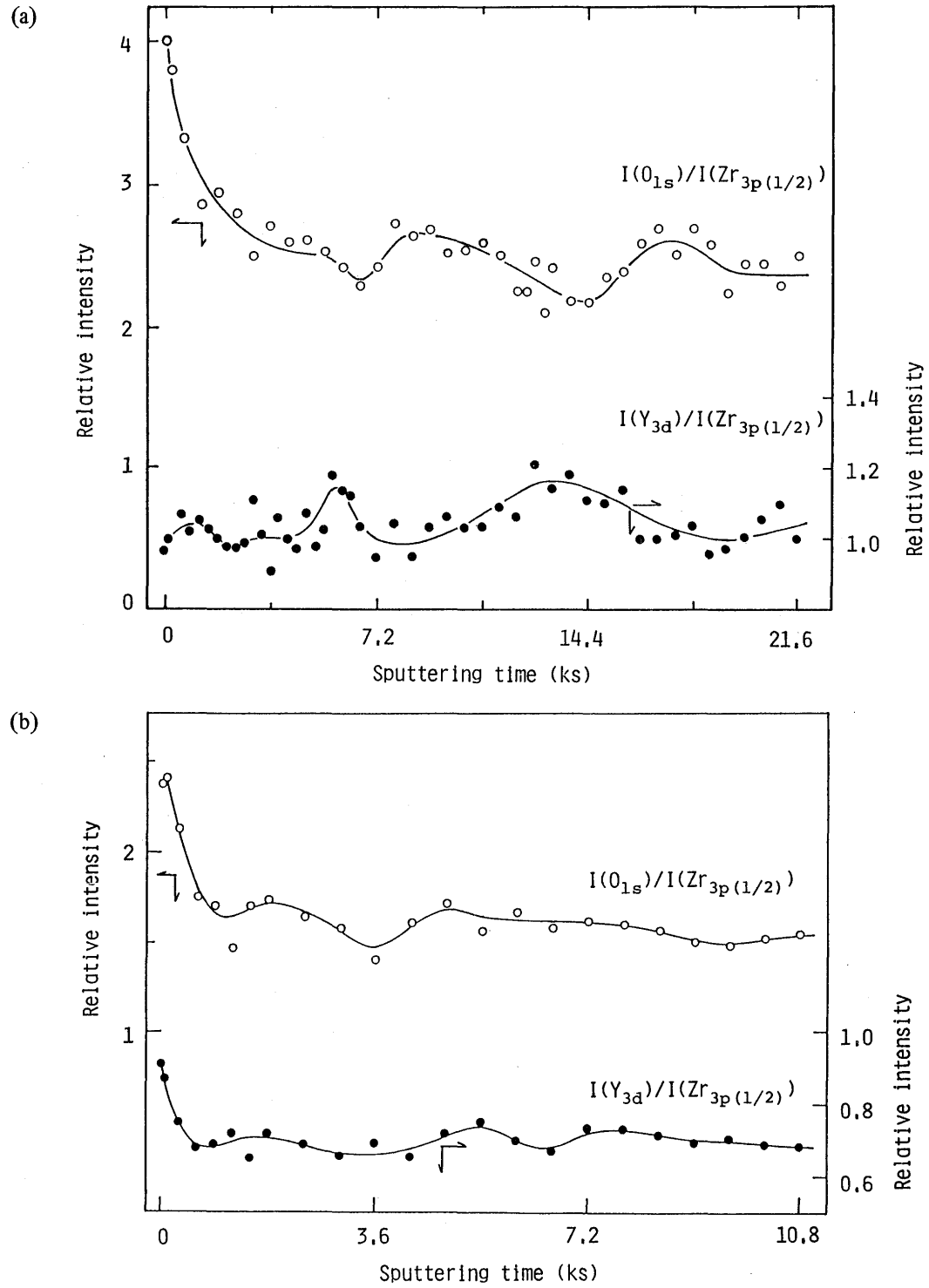

Fig. 3 Depth profiles of sprayed YSZ before and after heat-treatment at 1500°C (1773 K)
(a) as-sprayed YSZ, (b) heat-treated YSZ

(1473 K) can enhance the stabilization of monoclinic zirconia by yttria. On the other hand, it is found in fig. 2 that monoclinic zirconia in the as-sprayed commercial CSZ is not stabilized by the same heat-treatment. The evidence shows that yttria is excellent stabilizer for plasma sprayed zirconia.

As shown in fig. 3, it is observed that the relative intensity $I(Y_{3d})/I(Zr_{3p(1/2)})$[=R(Y)] in the as-sprayed YSZ is inclined to increase with decreasing the relative intensity R(O). It is shown from the result that the ratio of oxygen to yttrium in as-sprayed YSZ depends on the position of a particle and, therefore, yttria content in a particle is not completely homogenized. The influence attributed to the heterogeneity of yttria is observed in the chemical

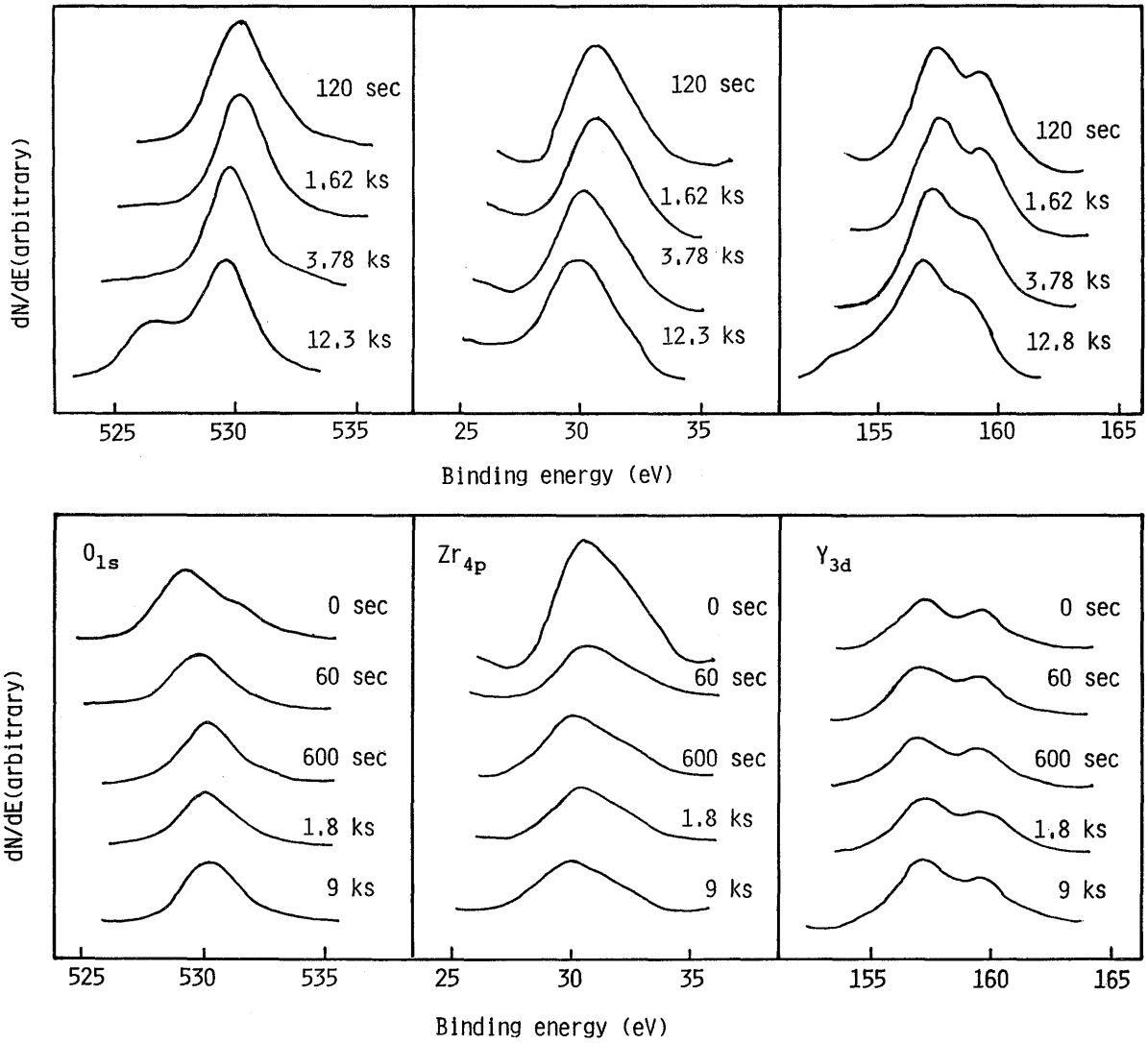

Fig. 4 O_{1s}, Y3d and Zr4p binding energies of (a) as-sprayed YSZ and (b) heat-treated YSZ.

shifts of O_{1s}, $Y_{3d(5/2)}$ and Zr_{4p} binding energies shift to lower energy, respectively, and the binding energy of $Y_{3d(5/2)}$ approaches to that of pure yttria (=156.4eV). This may be attributable to incomplete dissolution of yttria into monoclinic zirconia during plasma spraying. Therefore, it is reasonable to consider that dependences of O_{1s}, $Y_{3d(5/2)}$ and Zr_{4p} binding energies on R(O) are attributed to the degree of stabilization of monoclinic zirconia by yttria. Further, it is supported that the hollow region in the depth profile of R(O) in as-sprayed YSZ corroesponds to a boundary between sprayed layers. Considering the value of $Y_{3d(5/2)}$ binding energy in the hollow region, yttria seems to be a fairly high content. The expectation is supported by auger micrographs of 110eV and 153eV peaks.

Yttrium and zirconium are well homogenized after heat-treatment at 1500°C (1773 K), as shown in fig. 5-(b), except surface region. The homogeneity of zirconium and yttrium in heat-treated YSZ is also supported by the dependences of chemical shifts of O_{1s}, $Y_{3d(5/2)}$ and Zr_{4p} binding energies upon sputtering time.

In the as-sprayed YSZ, as indicated above, O_{1s} binding energy depends on R(O) value and two O_{1s} peaks were observed after sputtering for 12.3ks (205 min). The splitting of O_{1s} peak in as-sprayed zirconia seems to be related to yttria-enriched region near surface of each grain. On the other hand, the splitting of O_{1s} peak was not observed irrespective of showing a fairly low R(O) value. One possibility for the splitting of O_{1s} peak is the reduction of yttria. According to Kim and Winograd[10], various oxides can be reduced to lower oxide or metal by ion sputtering. The reduction of zirconium oxide is less possible according to the previous results[11] but we have no data for yttrium oxide. Besides, the splitting of O_{1s} peak is observed in the region with higher R(Y) value. Therefore, it is reasonable to attribute the splitting of O_{1s} peak to the reduction of yttria if the reduction cause to the splitting.

As sprayed x 300
Electron energy 110 eV

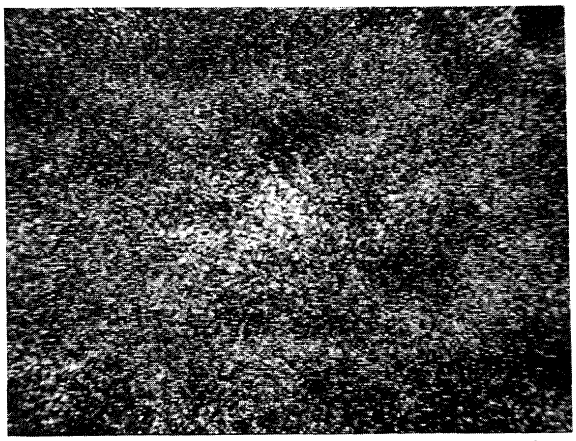

x 300
Heat treatment 1500°C, air 100 hr (20 hr x 5)
Electron energy 140 eV

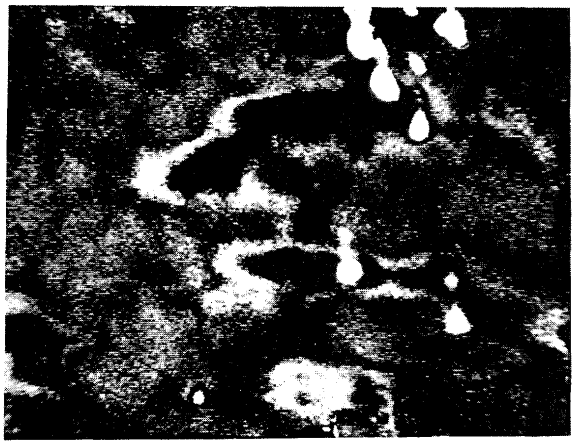

As sprayed x 300
Electron energy 153 eV

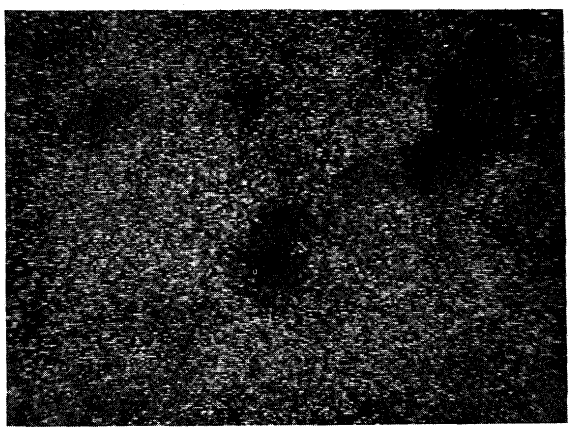

x 300
Heat treatment 1500°C, air 200 hr (20 hr x 10)
Electron energy 140 eV

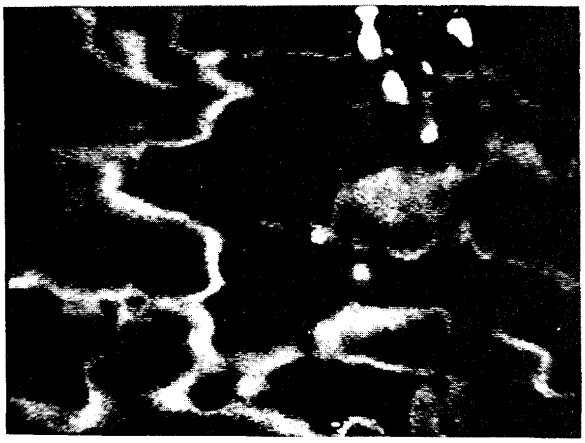

As sprayed x 300
Electron energy 177 eV

Fig. 5 Auger micrographs of as-sprayed and heat-treated YSZs.

Another possibility for the splitting is the structure of yttria because yttria contains fairly amount of anion vacancies [12]. The partial charge of a noticed anion increases by coordinating with a cation having small electronegativity, that is, the high electron donation of nearest neighbor cation. Further, the donating power of cation to anion is affected by the existence of anion vacancy (in this case, oxygen vacancy). Thus, the existence of oxygen vacancy in yttria may produce two sort of oxygen states. Taking into account the position of O_{1s} peak in lower

energy side, it may be reasonable to attribute the appearance of two O_{1s} peaks to the reduction of yttrium oxide. XPS study on pure yttrium oxide should be performed in further investigation.

5. Summary

Microstructure of plasma-sprayed YSZ was investigated by XPS and SAM. Heterogeneity of yttrium was observed in the as-sprayed YSZ. The heterogeneity of yttrium disappeared after heat-treatment at 1500°C (1773 K). Binding energies of O_{1s}, Y_{3d} and Zr_{4p} strongly depend on the heterogeneity of yttrium and the splitting of O_{1s} peak was also observed at the sputtering time of 12.3 ks (205 min). The splitting of O_{1s} peak may be attributed to the reduction of yttria. In plasma-sprayed YSZ heat-treated at 1500°C (1773 K), only week dependences of chemical shifts of O_{1s}, Y_{3d} and Zr_{4p} peaks were obtained and homogeneous distribution of zirconium was detected by auger micrographs.

Acknowledgement

The authors wish to thank Mr. N. Sasao and H. Funasaka (Tokai Works, Power Reactor and Nuclear Fuel Development Corporation) for measurement of scanning Auger micrograph.

References

1) G.McDonald and R.C. Hendricks, Thin Solid Films, **73** (1980) 491.
2) H.W. Grünling and K. Schneider, ibid., **84** (1981) 1.
3) T.A. Taylor, M.P. Overs, J.M. Quets and R.C. Tucker, Jr., ibid., **107** (1983) 427.
4) J. Stringer, I.M. Allam and D.P. Whittle, ibid., **45** (1977) 377.
5) C.C. Berndt and R.A. Miller, ibid. **119** (1984) 173.
6) J.G. Smeggil, A.W. Funkenbusch and N.S. Bornstein, ibid., **119** (1984) 327.
7) J.R. Hellmann and V.S. Stubican, J. Amer. Ceram Soc., **66** (1983) 260.
8) V.S. Stubican and S.P. Ray, ibid., **60** (1977) 534.
9) C. Pascual and P. Duran, ibid., **66** (1983) 23.
10) K.S. Kim and N. Winograd, Surface Science, **43** (1974) 625.
11) H.J. Mathieu, "Thin Film and Depth Profile Analysis", Ed. by H. Oechsner, Chap. 3, p. 39, Springer-Verlag, Berlin (1984).
12) D. Steele and B.E.F. Fender, J. Phys. C, 7 (1974) 1.